CrossMark

J. Plasma Physics (2015), *vol.* 81, 905810311 © Cambridge University Press 2015
doi:10.1017/S0022377815000033

Dispersion relation and growth rate in a free-electron laser with a background plasma

T. Mohsenpour[1]† and B. Maraghechi[2]

[1]Department of Physics, Faculty of Basic Sciences, University of Mazandaran, P. O. Box 47416-95447, Babolsar, Iran
[2] Department of Physics, Amirkabir University of Technology, P.O. Box 15875-4413, Tehran, Iran

(Received 13 June 2014; revised 2 January 2015; accepted 2 January 2015;
first published online 4 February 2015)

The method of perturbation has been applied to derive a general dispersion relation for a free-electron laser (FEL) with background plasma and helical wiggler in the presence of an axial magnetic field. This dispersion relation is solved numerically to find unstable interactions among all of the wave modes. Numerical calculations show that new coupling between the left wave and positive-energy space-charge of electron beam are found when wiggler induced velocity is large. This coupling does not change with increasing the plasma density. The growth rate of FEL is changed with increasing the plasma density and the normalized axial magnetic field.

1. Introduction

In its fundamental concept, the FEL is an extremely adaptable light source which can produce high-power coherent radiation virtually across the entire electromagnetic spectrum. The radiation is produced by an interaction among three constituents; (1) the relativistic electron beam, (2) an electromagnetic wave traveling in the same direction as the electrons, and (3) a periodic magnetic field (wiggler). In order to focus the electron beam, in the Raman regime, an axial magnetic field is usually employed.

The effects of background plasma on the interaction of electrons with the electromagnetic waves have been of considerable interest. There are many theoretical and experimental studies on the effects of background plasma, including FEL (Wen-Bing and Ya-Shen 1988; Tripathi and Liu 1990; Serbeto and Alves 1993; Sharma and Tripathi 1993; Pant and Tripathi 1994a, 1994b; Qian et al. 1994; Petrillo et al. 1995; Agarwal et al. 1996; Sharma and Tripathi 1996; Parashar et al. 1997; Seo and Choi 1997; Tsui and Serbeto 1998; Petrillo and Maroli 2000; Yang et al. 2002; Shi et al. 2003; Liu et al. 2004; Babaei and Maraghechi 2007, 2008; Nadrifard et al. 2013), gyrotrons (Schunemann and Zaginaylov 2001; Zaginaylov et al. 2006), and a dielectric Cherenkov maser (Shokri et al. 2000). The linear dispersion relation and the nonlinear evolution equation of the FEL in one-dimensional wiggler approximation are derived in Wen-Bing and Ya-Shen (1988). Babaei and Maraghechi (Babaei and Maraghechi 2007, 2008) studied the velocity spread and thermal effects of the beam electrons in FEL with background plasma. Ghazavi et al. (2010) derived the dispersion relation without considering the left circularly polarized electromagnetic wave, therefore, did not find the coupling between the space-charge wave and the left circular waves.

† Email address for correspondence: mohsenpour@umz.ac.ir

https://doi.org/10.1017/S0022377815000033 Published online by Cambridge University Press

The dispersion relation in Ghazavi et al. (2010) is to second order in the wiggler amplitude.

The purpose of the present study is to derive a dispersion relation of the right and left circularly polarized electromagnetic waves and the space charge wave for a FEL with background plasma. This dispersion relation is solved numerically to investigate the unstable interaction among many wave modes. For the coupling between the right and the space charge waves, these waves are resonant, and their amplitude increases, but the left wave is non-resonant, and its amplitude does not change. When the left wave is non-resonant, its contribution can be neglected in the dispersion relation and in the analysis and numerical solution. For the coupling between the left wave and the space-charge wave, the right wave is non-resonant, and its amplitude is unchanged and therefore plays an unimportant role in the coupling. Therefore, the contribution of the right wave in the dispersion relation can be neglected in the analysis and numerical solutions. In this paper, the dispersion relation of the two waves is not separately investigated (for example the left and the right waves or the right and the space charge waves). A new method has been used in which all possible wave modes can have unstable couplings with each other. By using this method, new unstable couplings have been found. In Sec. 2, the steady-state electron trajectories are found. In Sec. 3, a nonlinear dispersion relation is derived. In Sec. 4, a numerical analysis is carried out to investigate the unstable couplings between the waves. In Sec. 5, concluding remarks are made.

2. Steady-state orbits

Consider a relativistic electron beam (with charge $-e$, rest mass m, and energy $\gamma\, m\, c^2$) moving in the z-direction through a background plasma and a helical wiggler magnetic field that is described by

$$\mathbf{B}_w = (B_w/\sqrt{2})\, \exp(-ik_w z)\, \hat{\mathbf{e}} + (B_w/\sqrt{2})\, \exp(ik_w z)\, \hat{\mathbf{e}}^*, \tag{1}$$

where $\hat{\mathbf{e}} = (\hat{\mathbf{x}} + i\, \hat{\mathbf{y}})/\sqrt{2}$, $k_{5b} = k_L^2 c^2 - \omega^2 - B_1 D_2 + \omega\, \omega_b^2 D_8$, $\hat{\mathbf{e}}_z = \hat{\mathbf{z}}$. Due to the low energy of the beam, an axial magnetic field ($B_{0z}\hat{\mathbf{z}}$) is used to guide the electron beam. The beam density and current are assumed to be sufficiently small that the effects of equilibrium self-electric and self-magnetic fields can be neglected. Moreover, for short-wavelength perturbation, the transverse spatial variations ($\partial/\partial x = \partial/\partial y = 0$) are neglected. The steady-state electron orbits can be obtained by solving the equation of motion which will yield a longitudinal velocity $v_{||}\hat{\mathbf{z}}$ and a transverse velocity $\mathbf{v}_w$,

$$\mathbf{v}_0 = \left(v_w/\sqrt{2}\right)\, \exp(-ik_w z)\, \hat{\mathbf{e}} + \left(v_w/\sqrt{2}\right)\, \exp(ik_w z)\hat{\mathbf{e}}^* + v_{||}\hat{\mathbf{e}}_z, \tag{2}$$

where

$$v_w = \frac{\Omega_w v_{||}}{\Omega_0 - k_w v_{||}}, \tag{3}$$

$\Omega_0 = eB_0/\gamma_0 m_0 c$, $\Omega_w = eB_w/\gamma_0 m_0 c$, and

$$\frac{1}{\gamma_0^2} = \left(1 - \frac{v_{||}^2}{c^2} - \frac{v_w^2}{c^2}\right). \tag{4}$$

Substituting (3) into (4) yields a quadratic polynomial in the axial velocity which may be solved for $v_{||}/c$. There are in general, four solutions for $v_{||}/c$ for any sets of parameters; only the three of them with $v_{||}/c > 0$, will be considered herein.

https://doi.org/10.1017/S0022377815000033 Published online by Cambridge University Press

The steady-state trajectories may be divided into two classes corresponding to the cases, in which: $\Omega_0 < k_w v_{||}$ referred to as the group I, and $k_{6p} = \frac{\omega \omega_p^2 (\gamma_0 A_2)}{B_3(\omega - \gamma_0 \Omega_0)}$, referred to as the group II orbits. For lower values of axial magnetic field, for the group II orbits, the quantity

$$\Phi = 1 - \frac{\gamma_{||}^2 (v_w^2 / v_{||}^2)\, \Omega_0}{\left[1 + (v_w^2 / v_{||}^2)\right] \Omega_0 - k_w v_{||}}, \tag{5}$$

(that is obtained from $dv_{||}/d\gamma$) is negative and the corresponding orbits are in a negative mass regime in which an increase in the electron energy gives rise to a decrease in axial velocity.

3. Dispersion relation

The parametric excitation of electrostatic and electromagnetic waves in a relativistic electron beam that is passing through a helical wiggler, an axial guide magnetic field, and a uniform and stationary background plasma with density n_p will be considered. The analysis will be based on the electron continuity equation

$$\frac{\partial (\gamma\, n)}{\partial t} + \nabla \cdot (n \gamma\, \mathbf{v}) = 0, \tag{6}$$

the cold-electron relativistic momentum equation

$$\frac{\partial \mathbf{v}}{\partial t} + \mathbf{v} \cdot \nabla \mathbf{v} = -\frac{e}{\gamma m_0} \left[\mathbf{E} - \frac{1}{c^2} \mathbf{v}\, \mathbf{v} \cdot \mathbf{E} + \frac{1}{c} \mathbf{v} \times \mathbf{B} \right], \tag{7}$$

and the wave equation

$$\nabla \times (\nabla \times \mathbf{E}) + \frac{1}{c^2} \frac{\partial^2 \mathbf{E}}{\partial t^2} = \frac{\partial}{\partial t} \frac{4 \pi e}{c^2}\, (n\, \gamma\, \mathbf{v}), \tag{8}$$

with $d\gamma/dt = -(e/mc^2)(\mathbf{v} \cdot \mathbf{E})$.

The perturbed state can be considered as the unperturbed state $n_{0b} = const.$, $\mathbf{v}_0$, and $\mathbf{B}_0 (= \mathbf{B}_w + B_{0z} \hat{\mathbf{z}})$ plus small perturbations δn_b, δn_p, $\delta \mathbf{v}$, $\delta \mathbf{E}$, and $\delta \mathbf{B}$. The perturbed state is assumed to consist of a longitudinal space-charge wave and the right and left circularly polarized electromagnetic waves, with all perturbed waves propagating in the positive z-direction. The perturbation quantities may be assumed as

$$\delta \mathbf{E}_R,\ \delta \mathbf{B}_R,\ \delta\, \mathbf{v}_{bR}, \delta\, \mathbf{v}_{pR} \sim \hat{\mathbf{e}} \exp\left[i\, (k_R z - \omega t)\right], \tag{9}$$

$$\delta \mathbf{E}_L,\ \delta \mathbf{B}_L,\ \delta\, \mathbf{v}_{bL}, \delta\, \mathbf{v}_{pL} \sim \hat{\mathbf{e}}^* \exp\left[i\, (k_L z - \omega t)\right], \tag{10}$$

$$\delta \mathbf{E}_z,\ \delta\, \mathbf{v}_{bz}, \delta\, \mathbf{v}_{pz}, \delta\, n_b, \delta\, n_p \sim \hat{\mathbf{e}}_z \exp\left[i\, (kz - \omega t)\right], \tag{11}$$

where $k_R = k - k_w$ and $k_L = k + k_w$. $\delta\, \mathbf{v}_b$, $\delta\, n_b$, $\delta\, \mathbf{v}_p$, and $\delta\, n_p$ are the axial velocities and density perturbations for the electron beam and background plasma, respectively. By substituting the perturbation quantities into (7), the components of the momentum

https://doi.org/10.1017/S0022377815000033 Published online by Cambridge University Press

equation for the electron beam will be found as

$$-i\left[\omega - k_R v_{||} - \Omega_0 + A_1\right]\tilde{v}_{bR} + \frac{e}{\gamma_0 m_0}\left(1 - \frac{v_w^2}{2c^2}\right)\tilde{E}_R - \frac{e}{\gamma_0 m_0}\frac{v_w^2}{2c^2}\tilde{E}_L - \frac{e}{\gamma_0 m_0}\frac{v_w v_{||}}{\sqrt{2}c^2}\tilde{E}_z$$
$$-i\frac{\gamma_0^2}{2c^2}(\Omega_0 v_w - \Omega_w v_{||})v_w\tilde{v}_{bL} - iA_2\tilde{v}_{bz} - \frac{ie}{\gamma_0 m_0 c}v_{||}\tilde{B}_R = 0, \tag{12}$$

$$-i\left[\omega - k_R v_{||} + \Omega_0 - A_1\right]\tilde{v}_{bL} + \frac{e}{\gamma_0 m_0}\left(1 - \frac{v_w^2}{2c^2}\right)\tilde{E}_L - \frac{e}{\gamma_0 m_0}\frac{v_w^2}{2c^2}\tilde{E}_R - \frac{e}{\gamma_0 m_0}\frac{v_w v_{||}}{\sqrt{2}c^2}\tilde{E}_z$$
$$+i\frac{\gamma_0^2}{2c^2}(\Omega_0 v_w - \Omega_w v_{||})v_w\tilde{v}_{bR} + iA_2\tilde{v}_{bz} + \frac{ie}{\gamma_0 m_0 c}v_{||}\tilde{B}_L = 0, \tag{13}$$

$$-i\left[\omega - kv_{||}\right]\tilde{v}_{bz} + \frac{e}{\gamma_0 m_0}\left(1 - \frac{v_{||}^2}{c^2}\right)\tilde{E}_z - \frac{e}{\gamma_0 m_0}\frac{v_{||}v_w}{\sqrt{2}c^2}\tilde{E}_R - \frac{e}{\gamma_0 m_0}\frac{v_{||}v_w}{\sqrt{2}c^2}\tilde{E}_L$$
$$-i\frac{\Omega_w}{\sqrt{2}}\tilde{v}_{bR} + i\frac{\Omega_w}{\sqrt{2}}\tilde{v}_{bL} - i\frac{ev_w}{\sqrt{2}\gamma_0 m_0 c}\tilde{B}_L + \frac{iev_w}{\sqrt{2}\gamma_0 m_0 c}\tilde{B}_R = 0, \tag{14}$$

and for the background plasma

$$-i\left[\omega - \gamma_0\Omega_0\right]\tilde{v}_{pR} + \frac{e}{m_0}\tilde{E}_R - i\frac{\gamma_0\Omega_w}{\sqrt{2}}\tilde{v}_{pz} = 0, \tag{15}$$

$$-i\left[\omega + \gamma_0\Omega_0\right]\tilde{v}_{pL} + \frac{e}{m_0}\tilde{E}_L + i\frac{\gamma_0\Omega_w}{\sqrt{2}}\tilde{v}_{pz} = 0, \tag{16}$$

$$-i\omega\tilde{v}_{pz} + \frac{e}{m_0}\tilde{E}_z - i\frac{\gamma_0\Omega_w}{\sqrt{2}}\tilde{v}_{pR} + i\frac{\gamma_0\Omega_w}{\sqrt{2}}\tilde{v}_{pL} = 0, \tag{17}$$

where

$$A_1 = \left[\frac{\gamma_0}{2c^2}(\Omega_0 v_w - v_{||}\Omega_w)v_w\right], \tag{18}$$

$$A_2 = k_w\frac{v_w}{\sqrt{2}} + \frac{\Omega_w}{\sqrt{2}} + i\frac{\gamma_0}{\sqrt{2}c^2}(\Omega_0 v_w - \Omega_w v_{||}). \tag{19}$$

We can replace $\tilde{B}_R$ and $\tilde{B}_L$ with $\tilde{E}_R$ and $\tilde{E}_L$ by using $\nabla \times \mathbf{E} = -(1/c)\partial\mathbf{B}/\partial t$. Using the continuity equation, the perturbed beam and plasma densities will be found as

$$\tilde{n}_b = \left(\frac{n_b k}{\omega - kv_{||}} - \frac{n_b\gamma_0^3 v_{||}}{c^2}\right)\tilde{v}_{bz}, \tag{20}$$

$$\tilde{n}_p = \frac{kn_p}{\omega}v_{pz}. \tag{21}$$

By (12)–(14), after some algebra operations, $\tilde{v}_{bR}$, $\tilde{v}_{bL}$, and $\tilde{v}_{bz}$ can be obtained in terms of $\tilde{E}_R$, $\tilde{E}_L$, and $\tilde{E}_z$. Similarly, using (15)–(16) components of the perturbed velocity for plasma in terms of components of the perturbed electric field are found. By substituting $\tilde{v}_{bz}$ into (20) and $\tilde{v}_{pz}$ into (21), the perturbed beam and plasma densities in terms of the components of the perturbed electric field are obtained.

https://doi.org/10.1017/S0022377815000033 Published online by Cambridge University Press

Substituting the perturbation quantities into (8), the components of the wave equation will be found as

$$k_R^2 \tilde{E}_R - \frac{\omega^2}{c^2}\tilde{E}_R = -i\frac{4\pi e\omega}{c^2}\left(\tilde{n}_b \frac{v_w}{\sqrt{2}} + n_b \tilde{v}_{bR} + n_p \tilde{v}_{pR}\right), \tag{22}$$

$$k_L^2 \tilde{E}_L - \frac{\omega^2}{c^2}\tilde{E}_L = -i\frac{4\pi e\omega}{c^2}\left(\tilde{n}_b \frac{v_w}{\sqrt{2}} + n_b \tilde{v}_{bL} + n_p \tilde{v}_{pL}\right), \tag{23}$$

$$-\frac{\omega^2}{c^2}\tilde{E}_z = -i\frac{4\pi e\omega}{c^2}(\tilde{n}_b v_{\|} + n_b \tilde{v}_{bz} + n_p \tilde{v}_{pz}). \tag{24}$$

Substituting the perturbed velocities and densities, in terms of the components of the perturbed electric field for the electron beam and background plasma, into (22)–(24), and after some algebraic manipulations, the system of equations will reduce to

$$(k_{1b} + k_{1p})\tilde{E}_R + (k_{2b} + k_{2p})\,\tilde{E}_L + (k_{3b} + k_{3p})\,\tilde{E}_z = 0, \tag{25}$$

$$(k_{4b} + k_{4p})\tilde{E}_R + (k_{5b} + k_{5p})\,\tilde{E}_L + (k_{6b} + k_{6p})\,\tilde{E}_z = 0, \tag{26}$$

$$\left[-B_2 D_1 + \frac{\omega_p^2\,(\gamma_0 A_2)}{\omega B_3\,(\omega - \gamma_0\Omega_0)}\right]\tilde{E}_R + \left[B_2 D_2 + \frac{\omega_p^2\,(\gamma_0 A_2)}{\omega B_3\,(\omega + \gamma_0\Omega_0)}\right]\tilde{E}_L + \left[1 + B_2 D_3 + \frac{\omega_p^2}{\omega B_3}\right]\tilde{E}_z = 0, \tag{27}$$

where k_{1b}, k_{1p}, k_{2b}, k_{2p}, k_{3b}, k_{3p}, k_{4b}, k_{4p}, k_{5b}, k_{5p}, k_{6b}, k_{6p}, B_2, B_3, D_1, D_2, D_3, and A_2 are defined in the Appendix.

The necessary and sufficient condition for a non-trivial solution is to have the determinant of coefficients in (25)–(27) equal to zero. Imposing this condition yields the dispersion relation

$$\left[-B_2 D_1 + \frac{\omega_p^2\,(\gamma_0 A_2)}{\omega B_3\,(\omega - \gamma_0\Omega_0)}\right]\{(k_{2b} + k_{2p})(k_{6b} + k_{6p}) - (k_{3b} + k_{3p})(k_{5b} + k_{5p})\} + \left[B_2 D_2 + \frac{\omega_p^2\,(\gamma_0 A_2)}{\omega B_3\,(\omega + \gamma_0\Omega_0)}\right]\{(k_{1b} + k_{1p})(k_{6b} + k_{6p}) - (k_{3b} + k_{3p})(k_{4b} + k_{4p})\} + \left[1 + B_2 D_3 + \frac{\omega_p^2}{\omega B_3}\right]\{(k_{1b} + k_{1p})(k_{5b} + k_{5p}) - (k_{2b} + k_{2p})(k_{4b} + k_{4p})\} = 0. \tag{28}$$

Equation (28) is the DR for the coupled electrostatic and electromagnetic waves propagating along a relativistic electron beams in the presence of a background plasma and a helical wiggler and an axial magnetic field.

The uncoupled dispersion relation of the right circularly polarized electromagnetic wave in the absence of the wiggler and the left and space charge waves is

$$k_R^2 c^2 - \omega^2 + \frac{\omega_b^2(\omega - k_R v_{\|})}{\omega - k_R v_{\|} - \Omega_0} + \frac{\omega\omega_p^2}{\omega - \gamma_0\Omega_0} = 0, \tag{29}$$

where $\omega_b^2 = 4\pi\, n_b e^2/\gamma_0 m_0$. Similarly, the uncoupled dispersion relation of the left circularly polarized electromagnetic wave in the absence of the wiggler and the right

https://doi.org/10.1017/S0022377815000033 Published online by Cambridge University Press

and space charge waves is

$$k_L^2 c^2 - \omega^2 + \frac{\omega_b^2(\omega - k_L v_{||})}{\omega - k_L v_{||} + \Omega_0} + \frac{\omega\omega_p^2}{\omega + \gamma_0 \Omega_0} = 0. \tag{30}$$

The uncoupled dispersion relation for the space charge wave in the absence of the wiggler and the left and right waves is

$$1 - \frac{\omega_b'^2}{\gamma_{||}^3 \left(\omega - k v_{||}\right)^2} - \frac{\omega_p^2}{\omega^2} = 0, \tag{31}$$

where $\omega_b'^2 = 4\pi n_b e^2/m_0$, $\omega_p^2 = 4\pi n_p e^2/m_0$ and $\gamma_{||}$ is relativistic factor in the absence of wiggler. This is the dispersion relation for the space-charge wave in the system consisting of the relativistic electron beam and the background plasma. The dispersion relation for space charge wave consists of three physical modes, i.e. the slow (negative energy) and fast (positive energy) modes ($Sc_{b\pm}$) supported by electron beam and the longitudinal electrostatic modes of the plasma ($Sc_{p\pm}$). The fast and slow space-charge modes ($Sc_{b\pm}$) move parallel and antiparallel to the motion of the electron beam, respectively, giving rise to the positive and negative energy modes. While, plasma space-charge modes ($Sc_{p\pm}$) move parallel and antiparallel to the z-axis, respectively.

4. Numerical analysis

In this section, we have numerically solved the dispersion relation (28) to study the unstable couplings among many modes in a relativistic electron beam immersed inside a helical wiggler with background plasma and an axial magnetic field. The parameters are $k_w = 2\,\mathrm{cm}^{-1}$, $n_0 = 10^{12}\,\mathrm{cm}^{-3}$, $\gamma_0 = 3$, and $B_w = 1\,\mathrm{kG}$. To find the unstable couplings we assume that the wave number is real and ω can become complex. It was found that instability is only possible through coupling between two modes in which real-valued dispersion curves of the two modes coincide, giving rise to an imaginary part to the wave number in the form of a complex-conjugate pair, one of which is unstable.

The imaginary part of the wave normalized frequency $\mathrm{Im}\,\omega/k_w c$ versus k/k_w for coupling between Sc_{b-} mode and Sc_{p+} mode, referred to herein as electrostatic instability, and the coupling between R_e and Sc_{b-} modes, called FEL instability, are shown in Fig. 1. The downshifted FEL instability starts from $k/k_w = 1.75$ to $k/k_w = 2.75$, the maximum growth rate occurs at $k/k_w \approx 2.05$ with $(\mathrm{Im}\,\omega/k_w c)_{\max} = 0.0775$ and the upshifted FEL instability is from $k/k_w \approx 8.62$ to $k/k_w = 14.5$; the maximum growth rate occurs at $k/k_w = 11.5$ with $(\mathrm{Im}\,\omega/k_w c)_{\max} = 0.0805$. The electrostatic instability in Fig. 1 starts at $k/k_w = 0$ and continues to $k/k_w = 1.55$ and the maximum growth rate occurs at $k/k_w = 1.1$ with $(\mathrm{Im}\,\omega/k_w c)_{\max} = 0.184$.

The growth rate of the FEL instability, for the $Sc_{b-} - R_e$ coupling, for $\Omega_0/k_w c = 0$, 0.1, 0.2, 0.3, 0.4, 0.52 is shown in Fig. 2. This figure shows how the FEL instability is affected by the changes in normalized cyclotron frequency $\Omega_0/k_w c$. At lower $\Omega_0/k_w c$, there are two separate instability regions. Increasing the normalized cyclotron frequency $\Omega_0/k_w c$ moves the dispersion curves of the escape mode to higher frequencies and the dispersion curves of the space-charge wave to the lower frequencies so that the intersection points, i.e. peaks with the same label, get closer as indicated in Fig. 2. Figure 2 also shows that increasing the normalized cyclotron frequency increases growth rate of the FEL coupling. It should be noted that, the coupling between the Sc_{b-} and the Sc_{p+} modes does not change when the normalized

https://doi.org/10.1017/S0022377815000033 Published online by Cambridge University Press

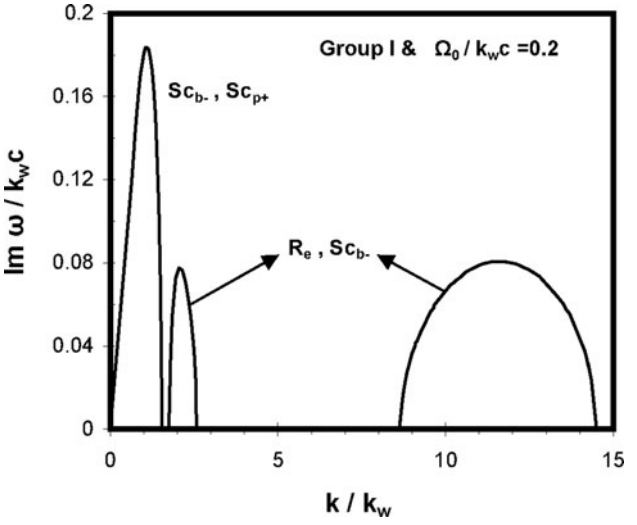


FIGURE 1. $\mathrm{Im}\,\omega/k_w c$ versus k/k_w for the group I orbits with $\Omega_0/k_w c = 0.2$ and $\omega_p/k_w c = 1.33$.

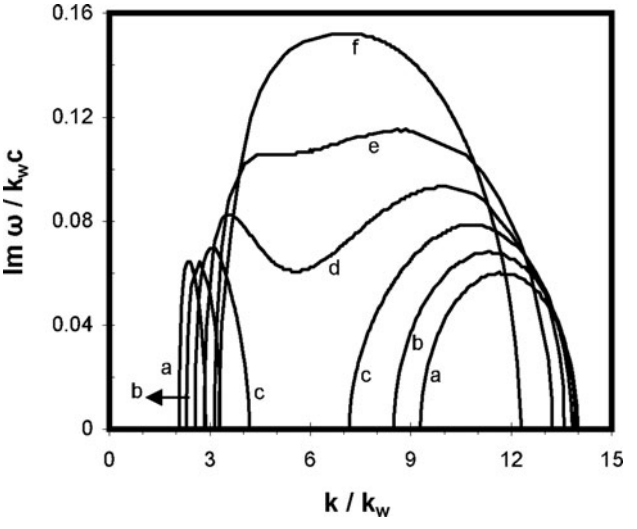


FIGURE 2. $\mathrm{Im}\,\omega/k_w c$ versus k/k_w for the $Sc_{b-} - R_e$ coupling, for $\Omega_0/k_w c = 0$ (a), 0.1(b), 0.2(c), 0.3(d), 0.4(e), 0.52(f).

cyclotron frequency is changed. It can be concluded that the normalized cyclotron frequency has no noticeable effect on the electrostatic instability. In Fig. 3, the effects of the background plasma density on the FEL and the electrostatic instabilities are shown. Figure 3 shows that increasing $\omega_p/k_w c$ moves the two separate peaks toward each other so that at larger $\omega_p/k_w c$ the two separate peaks merge into a single peak. Also, Fig. 3 shows that increasing the plasma density, up to a certain value, increases the growth rate of the FEL instability. If the plasma density is increased further the growth rate is decreased to zero at a critical density, as shown in Fig. 3. For the coupling between Sc_{b-} and Sc_{p+} modes the growth rate increases with increasing plasma density.

For the larger values of the normalized cyclotron frequency, in group I orbits, where the transverse wiggler motion is large, we should expect couplings between

https://doi.org/10.1017/S0022377815000033 Published online by Cambridge University Press

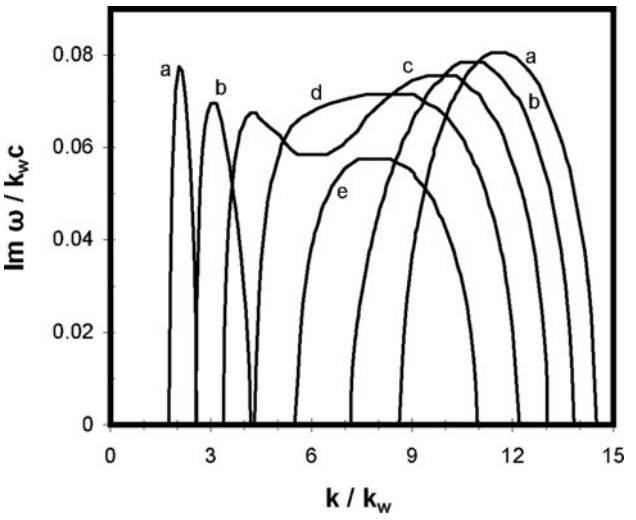


FIGURE 3. $\mathrm{Im}\,\omega/k_w c$ versus k/k_w for the $Sc_{b-} - R_e$ coupling of the group I orbits and for different $\omega_p/k_w c$.

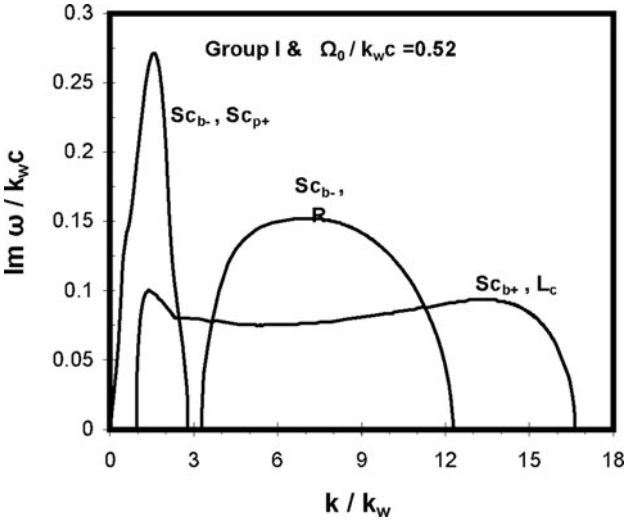


FIGURE 4. $\mathrm{Im}\,\omega/k_w c$ versus k/k_w for the group I orbits with $\Omega_0/k_w c = 0.52$ and $\omega_p/k_w c = 1.33$.

other modes in which relativistic terms play a more important role. Coupling between the left-cyclotron (L_c) and the positive-energy space-charge wave (Sc_{b+}), supported by the electron beam, are found for the large values of $\Omega_0/k_w c$ in the group I orbits. $\mathrm{Im}\,\omega/k_w c$ versus k/k_w for the coupling between L_c and Sc_{b+} modes is shown in Fig. 4 with $\Omega_0/k_w c = 0.52$ and $\omega_p/k_w c = 1.33$. This coupling starts at $k/k_w = 0.948$ and ends at $k/k_w = 16.63$ in Fig. 4.

Coupling between the right-cyclotron (R_c) and the negative-energy space-charge wave (Sc_{b-}), supported by the electron beam, and the electrostatic instability, for the group II orbits with $\Phi > 0$, are shown in Fig. 5 with $\Omega_0/k_w c = 1.6$ and $\omega_p/k_w c = 1.33$. Coupling between R_c and Sc_{b-} modes starts from $k/k_w = 1.97$ and ends at $k/k_w = 2.33$ and again starts at $k/k_w = 7.43$ and ends at $k/k_w = 13.21$. The electrostatic instability

https://doi.org/10.1017/S0022377815000033 Published online by Cambridge University Press

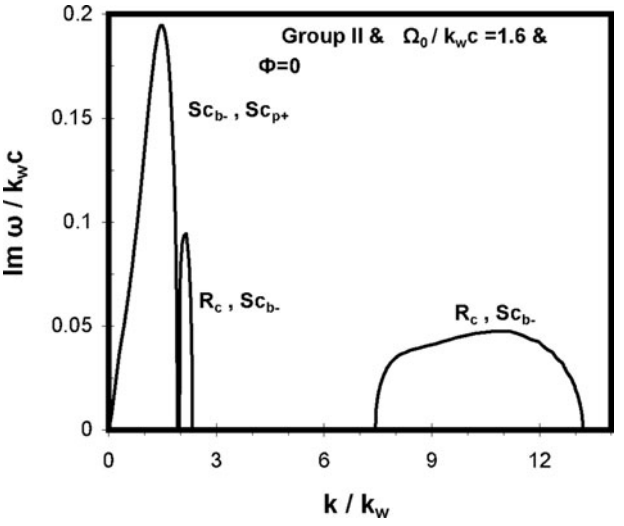


FIGURE 5. $\mathrm{Im}\,\omega/k_w c$ versus k/k_w for the group II orbits with $\Phi > 0$.

starts from $k/k_w = 0$ and ends at $k/k_w = 1.91$ in Fig. 5 with $(\mathrm{Im}\,\omega/k_w c)_{\max} = 0.195$ at $k/k_w = 1.48$.

For the group II orbits in the negative mass regime the wiggler induced velocity v_w is large as a result, we should expect couplings between other modes in which relativistic terms play a more important. In Fig. 6, the coupling between the right-cyclotron (R_c) and the negative-energy space-charge wave (Sc_{b-}), supported by the electron beam, coupling between the negative space-charge waves (Sc_{b-}), supported by the electron beam, and the plasma mode (Sc_{p+}), supported by the background plasma, and coupling between Sc_{b+} mode and the left-cyclotron (L_c) are shown with $\Omega_0/k_w c = 1.2$ and $\omega_p/k_w c = 1.33$. The electrostatic instability starts at $k/k_w = 0.735$ and ends at $k/k_w = 2.363$ with $(\mathrm{Im}\,\omega/k_w c)_{\max} = 0.22$ at $k/k_w = 1.84$. The FEL instability starts from $k/k_w = 6.08$ and continues to $k/k_w = 9.72$ with $(\mathrm{Im}\omega/k_w c)_{\max} = 0.0965$ at $k/k_w = 7.55$. The coupling between Sc_{b+} and L_c modes occurs in the range $0.94 < k/k_w < 5.50$ and $k/k_w > 11.01$.

When two wave modes are in resonance, their amplitude increases while the amplitude of a non-resonant mode remains unchanged. For coupling between the R_e and Sc_{1-} modes, the right and the space-charge waves are resonant, and their amplitude increases, but the left wave is non-resonant, and its amplitude does not change. Since the left wave is non-resonant, its contribution can be neglected in the DR (28), and in the analysis and numerical solution. If $\tilde{E}_L$ is neglected in, (25)–(27), we can obtain the dispersion relation for the right and the space-charge waves. For the coupling between the left wave and the space-charge wave, the right wave is non-resonant, and its amplitude is unchanged and therefore plays an unimportant role in the coupling. Therefore, the contribution of the right wave in the DR (28) can be neglected in the analysis and numerical solutions. In (25)–(27), if we consider $\tilde{E}_R = 0$, we can obtain a dispersion relation for the left and the space-charge waves. In this case, we have found a new unstable coupling. In the present paper, the dispersion relation of two waves are not separately investigated (for example the left and the right waves or the right and the space-charge). A new method has been used in which all possible wave modes can have unstable couplings with each other. By using this method, new unstable couplings have been found.

https://doi.org/10.1017/S0022377815000033 Published online by Cambridge University Press

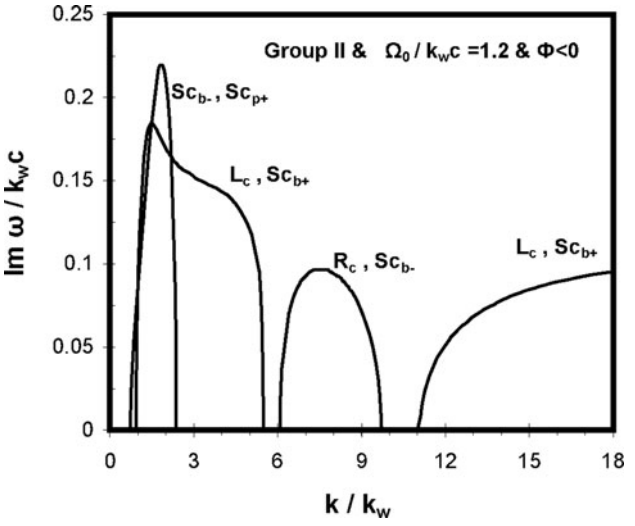


FIGURE 6. Im $\omega/k_w c$ versus k/k_w for the group II orbits with $\Phi < 0$.

5. Conclusion

In this paper, a general dispersion relation (28) is derived for a FEL with background plasma and helical wiggler in the presence of an axial magnetic field. In the dispersion relation, all of the relativistic terms related to the transverse wiggler motion are included. In order to study many unstable couplings among all possible modes, the dispersion relation (28) is solved numerically. Our results show that by increasing the plasma density the growth rate of electrostatic instability is increased and the bandwidth of its unstable spectrum is widened. This instability does not change when the normalized axial magnetic field is increased. It should be noted that the electrostatic instability is due to the interaction of two longitudinal motions associated with the space charge wave supported by the electron beam and plasma. We should therefore expect that the axial magnetic field and the resulting transverse velocity not to influence the electrostatic instability.

For lower values of the normalized axial magnetic field, in the group I orbits there exist only the main FEL coupling between the right wave and the negative-energy space-change wave of the electron beam and electrostatic instability, while for higher fields, when ν_w is large, new couplings are found between the left wave and the positive-energy space-charge wave of the beam. Our numerical results show that when the plasma density is increased, up to certain value, the growth rate of the FEL coupling increases, however, if the plasma density is increased further the growth rate decreases to zero at a critical density. Also, our numerical results show that increasing the electron beam density causes the critical plasma density to decrease. It is important to note that when plasma density increases the growth rate of the coupling between the Sc_{b+} and the L_c modes does not change considerably. The effects of plasma density on the couplings can be described physically as follows. In the absence of background plasma, the uncoupled dispersion relation for the space charge wave of electron beam is $(\omega - k\, v_{||})^2 = \omega_b^2\, \gamma_{||}^{-2}$ and the phase velocities of the positive and the negative energy space-charge modes are $\omega/k = v_{||} + \omega_b/\gamma_{||}k$ and $\omega/k = v_{||} - \omega_b/\gamma_{||}k$, respectively. In the presence of the background plasma, the phase velocities of the positive and negative energy space-charge waves of the electron beam depend on the plasma density. With increasing the plasma density the phase velocity of the Sc_{b-}

https://doi.org/10.1017/S0022377815000033 Published online by Cambridge University Press

mode is decreased and the phase velocity of the Sc_{b+} mode is increased. On the other hand, the phase velocities of the Sc_{b-} mode and the plasma mode approach each other and can interact with one another while the phase velocity of the Sc_{b-} mode and the plasma mode move apart and cannot interact with each other.

Electrostatic instability is due to the interaction of two longitudinal motions associated with the negative energy space-charge mode on the electron beam with the electrostatic modes of the plasma. Therefore, we should expect the wiggler induced transverse motion, not to influence the two-stream instability.

Appendix: Definition of quantities

The following quantities are used in (25)–(27):

$$D_1 = \{[A_R A_8 + A_5 A_1]\ [A_2 (A_8 - A_5)] - (A_8 A_7 + A_5^2)\ A_8\ (A_2 A_1 - k_R A_3 \omega^{-1} - A_4)\}\ A_9^{-1}, \tag{A1}$$

$$D_2 = \{[A_R A_5 + A_8 A_1]\ [A_2 (A_8 - A_5)] - (A_8 A_7 + A_5^2)\ A_L A_2 + (k_L A_3 \omega^{-1} - A_4)\ A_8\}\ A_9^{-1}, \tag{A2}$$

$$D_3 = [A_2 A_4 (A_8 - A_5)^2 - (A_8 A_7 + A_5^2)\ (A_2 A_4 - A_8 \gamma_{||}^{-2})]\ A_9^{-1}, \tag{A3}$$

$$D_4 = [A_R A_8 + A_5 A_1 - D_1 A_6 (A_8 + A_5)]\ (A_8 A_7 + A_5^2)^{-1}, \tag{A4}$$

$$D_5 = [A_R A_5 + A_8 A_1 - D_1 A_6 (A_8 + A_5)]\ (A_8 A_7 + A_5^2)^{-1}, \tag{A5}$$

$$D_6 = [A_4 (A_8 - A_5) - D_3 A_6 (A_8 + A_5)]\ (A_8 A_7 + A_5^2)^{-1}, \tag{A6}$$

$$D_7 = A_5^{-1}\ [A_7 D_4 + A_6 D_1 - A_R], \tag{A7}$$

$$D_8 = A_5^{-1}\ [A_7 D_5 + A_6 D_2 - A_1], \tag{A8}$$

$$D_9 = A_5^{-1}\ [A_7 D_6 + A_6 D_3 - A_4], \tag{A9}$$

$$A_1 = \frac{v_w^2}{2c^2}, \tag{A10}$$

$$A_2 = \frac{\Omega_w}{\sqrt{2}}, \tag{A11}$$

$$A_3 = \frac{v_w}{\sqrt{2}c}, \tag{A12}$$

$$A_4 = \frac{v_w v_{||}}{\sqrt{2}c^2}, \tag{A13}$$

$$A_5 = \frac{\gamma_0^2 v_w}{2c^2}(\Omega_0 v_w - \Omega_w v_{||}), \tag{A14}$$

$$A_6 = \frac{k_w v_w}{\sqrt{2}} + \frac{\Omega_w}{\sqrt{2}c} + \frac{\gamma_0^2}{\sqrt{2}c^2}(\Omega_0 v_w - \Omega_w v_{||}) v_{||}, \tag{A15}$$

$$A_7 = \omega - k_R v_{||} - \Omega_0 + A_5, \tag{A16}$$

$$A_8 = \omega - k_L v_{||} + \Omega_0 - A_5, \tag{A17}$$

$$A_9 = \left\{(A_8 A_7 + A_5^2)\left[\frac{A_6 \Omega_w}{\sqrt{2}} + A_8(\omega - k_L v_{||})\right] + (A_8 - A_5)\frac{A_6 A_8 \Omega_w}{\sqrt{2}}\right\}, \tag{A18}$$

$$A_R = \left(1 - \frac{v_{wj}^2}{2c^2} - \frac{k_R v_{||j}}{\omega}\right), \tag{A19}$$

https://doi.org/10.1017/S0022377815000033 Published online by Cambridge University Press

$$A_L = \left(1 - \frac{v_{wj}^2}{2c^2} - \frac{k_L v_{||j}}{\omega}\right), \tag{A20}$$

$$k_{1b} = k_R^2 c^2 - \omega^2 + B_1 D_1 + \omega\omega_b^2 D_4, \tag{A21}$$

$$k_{1p} = \frac{\omega\omega_p^2}{\omega + \gamma_0\Omega_0}\left(1 + \frac{(\gamma_0 A_2)^2}{B_3(\omega + \gamma_0\Omega_0)}\right), \tag{A22}$$

$$k_{2b} = B_1 D_2 - \omega\omega_b^2 D_5, \tag{A23}$$

$$k_{2p} = -\frac{\omega\omega_p^2(\gamma_0 A_2)^2}{B_3\left(\omega^2 - \gamma_0^2\Omega_0^2\right)}, \tag{A24}$$

$$k_{3b} = -B_1 D_3 - \omega\omega_b^2 D_6, \tag{A25}$$

$$k_{3p} = -\frac{\omega\,\omega_p^2(\gamma_0 A_2)}{B_3(\omega + \gamma_0\Omega_0)}, \tag{A26}$$

$$k_{4b} = B_1 D_1 - \omega\omega_b^2 D_7, \tag{A27}$$

$$k_{4p} = -\frac{\omega\,\omega_p^2(\gamma_0 A_2)^2}{B_3\left(\omega^2 - \gamma_0^2\Omega_0^2\right)}, \tag{A28}$$

$$k_{5b} = k_L^2 c^2 - \omega^2 - B_1 D_2 + \omega\,\omega_b^2 D_8, \tag{A29}$$

$$k_{5p} = \frac{\omega\omega_p^2}{\omega - \gamma_0\Omega_0}\left(1 + \frac{(\gamma_0 A_2)^2}{B_3(\omega - \gamma_0\Omega_0)}\right), \tag{A30}$$

$$k_{6b} = -B_1 D_3 + \omega\omega_b^2 D_9, \tag{A31}$$

$$k_{6p} = \frac{\omega\,\omega_p^2(\gamma_0 A_2)}{B_3(\omega - \gamma_0\Omega_0)}, \tag{A32}$$

$$B_1 = k\,A_3\frac{\omega\omega_b^2}{(\omega - k v_{||})}, \tag{A33}$$

$$B_2 = \frac{\omega_b^2}{(\omega - k v_{||})}, \tag{A34}$$

$$B_3 = \left[\omega - (\gamma_0 A_2)^2\left(\frac{2\omega}{\omega^2 - \gamma_0^2\Omega_0^2}\right)\right], \tag{A35}$$

REFERENCES

Agarwal, R. N., Ghanshyam, Tripathi V. K. and Agarwal, P. C. 1996 *IEEE Trans. Plasma Sci.* **24**, 1197.

Babaei, S. and Maraghechi, B. 2007 *Phys. Plasmas* **14**, 053 114.

Babaei, S. and Maraghechi, B. 2008 *Phys. Plasmas* **15**, 1.

Ghazavi, A., Maraghechi, B. and Mohsenpour, T. 2010 *Phys. Plasmas* **108**, 123 302.

Liu, W., Yang, Z. and Liang, Z. 2004 *Int. J. Infrared Millim. Waves* **25**, 1053.

Nadrifard, S. Maraghechi, B. and Mohsenpour, T. *Plasma Phys. Control. Fusion* **55,** 025 012.

Pant, K. K. and Tripathi, V. K. 1994a *IEEE Trans. Plasma Sci.* **22**, 217.

Pant, K. K. and Tripathi, V. K. 1994b *Phys. Plasmas* **1**, 1025.

Parashar, J., Pandey, H. D., Sharma, A. K. and Tripathi, V. K. 1997 *J. Plasma Phys.* **58**, 613.

Petrillo, V. and Maroli, C. 2000 *Phys. Rev.* E **62**, 8612.

Petrillo, V., Serbeto, A., Maroli, C., Parrella, R. and Bonifacio, R. 1995 *Phys. Rev.* E **51**, 6293.

Qian, B., Liu, Y. and Li, C. 1994 *Phys. Plasmas* **1**, 4089.

https://doi.org/10.1017/S0022377815000033 Published online by Cambridge University Press

Schunemann, K. and Zaginaylov, G. I. 2001 *Frequenz* **55**, 252.
Seo, Y. and Choi, E. H. 1997 *IEEE Trans. Plasma Sci.* **25**, 360.
Serbeto, A. and Alves, M. V. 1993 *IEEE Trans. Plasma Sci.* **21**, 243.
Sharma, A. and Tripathi, V. K. 1993 *Phys. Fluids* B **5**, 171.
Sharma, A. and Tripathi, V. K. 1996 *Phys. Plasmas* **3**, 3116.
Shi, Z., Yang, Z. and Liang, Z. 2003 *Int. J. Infrared Millim. Waves* **24**, 1823.
Shokri, B., Ghomi, H. and Latifi, H. 2000 *Phys. Plasmas* **7**, 2671.
Tripathi, V. K. and Liu, C. S. 1990 *IEEE Trans. Plasma Sci.* **18**, 466.
Tsui, K. H. and Serbeto, A. 1998 *Phys. Rev.* E **58**, 5013.
Wen-Bing, P. and Ya-Shen, C. 1988 *Int. J. Electron.* **65**, 551.
Yang, Z., Chen, H. and Liang, Z. 2002 *Int. J. Infrared Millim. Waves* **23**, 1057.
Zaginaylov, G. I., Shcherbinin, V. I., Schuenemann, K. and Thumm, M. K. 2006 *IEEE Trans. Plasma Sci.* **34**, 512.

https://doi.org/10.1017/S0022377815000033 Published online by Cambridge University Press